

# Improved post-processing strategy for MOLLI based tissue characterization allows application in patients with dyspnoe and impaired left ventricular function

Thomas Kampf<sup>1,3,4</sup>, Wolfgang Rudolf Bauer<sup>2,3,4</sup>, Theresa Reiter<sup>2,3,\*</sup>

<sup>1</sup> University of Wuerzburg, Department for Experimental Physics V, Am Hubland, 97074 Wuerzburg, Germany

<sup>2</sup> University Hospital Wuerzburg, Department of Internal Medicine I, Oberduerrbacher Straße 6a, 97080 Wuerzburg, Germany

<sup>3</sup> Comprehensive Heart Failure Centre Wuerzburg, Germany

Received 14 November 2016; accepted 13 July 2017

## Abstract

Contrast and non-contrast MRI based characterization of myocardium by  $T_1$ -mapping will be of paramount importance to obtain biomarkers, e.g. fibrosis, which determines the risk of heart failure patients.

$T_1$ -mapping by the standard post-processing of the modified look-locker inversion recovery (MOLLI) lacks of accuracy when trying to reduce its duration, which on the other hand, is highly desirable in patients with heart failure. The recently suggested inversion group fitting (IGF) technique, which considers more parameters for fitting, has a superior accuracy for long  $T_1$  times despite a shorter duration. However, for short  $T_1$  values, the standard method has a superior precision. A conditional fitting routine is proposed which ideally takes advantage of both algorithms.

**Materials and methods:** All measurements were performed on a 1.5 T clinical scanner (ACHIEVA, Philips Healthcare, The Netherlands) using a MOLLI 5(n)3(n)3 prototype with  $n$ (heart beats) being a variable waiting time between inversion experiments. Phantom experiments covered a broad range of  $T_1$  times, waiting times and heart rates. A saturation recovery experiment served as a gold standard for  $T_1$  measurement. All data were analyzed with the standard MOLLI, the IGF fit and the conditional fitting routine and the obtained  $T_1$  values were compared with the gold standard. In vivo measurements were performed in a healthy volunteer and a total of 34 patients with normal findings, dilative cardiomyopathy and amyloidosis.

**Results:** Theoretical analysis and phantom experiments provided a threshold value for an apparent IGF  $T_1^*$  determining processing with IGF post processing for values above, or switching to the standard technique for values below. This was validated in phantoms and patients measurements. A reduction of the waiting time to 1 instead of 3 heart beats between the inversion experiments showed reliable results. The acquisition time was reduced from 17 to 13 heart beats. The in vivo measurements showed ECV values between 25% (18–33%; SD 0.03) in the healthy, 30% (22–40%; SD 0.04) in patients with DCM and 45% (30–60%; SD 0.9) in patients with amyloidosis.

**Conclusion:** The adopted post-processing algorithm determines long  $T_1$  values with high accuracy and short  $T_1$  values while maintaining a high precision. Based on reduction of waiting time, and independence of heart rate, it shortens breath hold duration and allows fast  $T_1$ -mapping, which is frequently a prerequisite in patients with cardiac diseases.

**Keywords:**  $T_1$ -mapping, ECV, MOLLI, Post-processing

*Abbreviations:* MOLLI, modified look locker inversion recovery; bSSFP, balanced Steady-State Free Precession; IGF, inversion group fitting; CA, contrast agent; ECG, electrocardiogram; SNR, signal-to-noise ratio;  $T_1$ , longitudinal relaxation time;  $T_1^*$ , apparent longitudinal relaxation time;  $M_{SS}$ , steady state magnetization;  $M_0$ , equilibrium magnetization;  $T_{RR}$ , time between two R-waves;  $M_{on}$ , initial magnetization for each inversion;  $T_{i,n}$ , inversion time of the  $i$ th image after the  $n$ th inversion pulse;  $S_i$ , measured signal of one inversion;  $A$ , fitting parameter, in this work equaling  $M_{SS}$ ;  $B_n$ , fitting parameter, in this work equaling  $M_{on}$ .

\*Corresponding author: Theresa Reiter, University Hospital Wuerzburg, Department of Internal Medicine I, Oberduerrbacher Straße 6a, 97080 Wuerzburg, Germany.

E-mail addresses: [Thomas.kampf@physik.uni-wuerzburg.de](mailto:Thomas.kampf@physik.uni-wuerzburg.de) (T. Kampf), [Bauer\\_w@ukw.de](mailto:Bauer_w@ukw.de) (W.R. Bauer), [Reiter\\_t@ukw.de](mailto:Reiter_t@ukw.de) (T. Reiter).

<sup>4</sup> Shared first authorship.

## Introduction

The biomarker extracellular volume of myocardium (ECV) in cardiac MRI functions as surrogate for the extracellular matrix and is linked to the clinical outcome. The increase of the ECV is associated with the short term cardiovascular mortality and in diseases such as amyloidosis and dilative cardiomyopathy (DCM), recent data show that the ECV is an independent predictor of mortality [1,2].

Cardiac magnetic resonance imaging (cMRI) allows the radiation free in vivo tissue characterization by using native and contrast enhanced sequences.  $T_1$  maps acquired with the modified look locker inversion recovery (MOLLI) sequence can quantify the ECV. MOLLI is based on a series of three inversions with multiple single shot balanced Steady-State Free Precession (bSSFP) readouts triggered to each heart-beat during the relaxation of longitudinal magnetization. This requires a sufficient waiting period in-between the inversions to guarantee recovery to full magnetization before the next inversion. In the original scheme, the waiting time covers three heart beats, which lengthens the necessary breath-hold to 17 heartbeats. A three parameter fit is applied to the acquired data [3,4]. The required breathing maneuvers demand an excellent patient compliance and condition to minimize co-registration artifacts, which limits the application of MOLLI in patients with dyspnea e.g. due to impaired systolic or diastolic cardiac function.

An optimized post-processing aims at the shortening of the routine MOLLI protocol by minimizing the waiting time between the inversions, improving accuracy and maintaining precision. One solution is to alleviate the constraint that equilibrium magnetization must be reached before the 2nd and 3rd inversion pulse by using the magnetization immediately after these pulses as additional fit parameters. This inversion group fitting (IGF) approach was recently suggested by Sussmann et al. [5] for determination of native  $T_1$  values and by us [6]. IGF has the advantage that its accuracy is independent from the waiting time in-between the inversion experiments, which is a prerequisite to gain sufficient accuracy for the standard MOLLI, in particular for long  $T_1$  times. However, the increased number of fitting parameters makes IGF susceptible to fitting errors implying a lower precision. This, we anticipated, should especially become a problem for smaller  $T_1$  values, when compared to the standard MOLLI, which would exclude IGF from a broad field of applications, e.g. determination of ECV.

Hence, in this paper we propose a technique, which combines the advantages of both approaches by a conditional fit in order to obtain the better precision of the standard MOLLI analysis for short  $T_1$  times, while gaining the advantage of the IGF method to obtain accurate long  $T_1$  times though a shortened acquisition time.

The paper is structured as follows: as IGF has solely been characterized for native (long)  $T_1$  values, we first systematically investigate its precision for a broad range of  $T_1$

phantoms and heart rates. The same is done for the accuracy of standard MOLLI post-processing. Based on error analysis we present a switching algorithm for either IGF or standard post-processing. This adaptive analysis is validated in phantoms and in patients with impaired cardiac function. Special emphasize is put on the dependence on the waiting period between the inversion recoveries and a reliable quantification for  $T_1$  times in myocardial tissue pre and post contrast agent (CA) administration, which is the base for ECV quantification.

## Theory

### MOLLI and IGF

The standard post-processing of MOLLI fits the signal intensity time curve to a single exponential function  $S(t) = A - Be^{-t/T_1^*}$  with fit parameters  $A$ ,  $B$  and the apparent relaxation time  $T_1^*$ .  $A$  denotes the steady state signal  $M_{ss}$  and  $B$  defines the dynamic range  $B = M_0 + M_{ss}$  with  $M_0$  as the equilibrium signal [7]. The longitudinal relaxation time is related to its fitting partner by

$$T_1 = \frac{M_0}{M_{ss}} T_1^* = \left( \frac{B}{A} - 1 \right) T_1^*. \quad (1)$$

For  $T_1$ -mapping, three consecutive inversion experiments are performed during a single breath hold. For each experiment, the inversion time is varied with respect to the ECG-gated image acquisition. In standard post-processing, data points from these inversion recoveries are merged and fitted as described above to obtain  $T_1$  from Eq. (1). This approach demands a sufficient long waiting time between the inversion experiments so that the subsequent inversion pulse acts on equilibrium magnetization.

The IGF method requires equilibrium magnetization only for the first inversion pulse. The subsequent inversion recoveries  $n$  are assigned an individual initial magnetization  $M_{0,n}$ , and, hence, fitting parameter  $B_n = M_{0,n} + M_{ss}$ . As there is no constraint to these parameters, the waiting periods can be shortened. The other parameters such as steady state signal  $M_{ss}$  (appearing in fitting parameter  $A$  and  $B_n$ ) and apparent relaxation time  $T_1^*$  remain unchanged for all inversion curves (see Fig. 1). The fit parameters are obtained from measured signal-time points  $(t_{i,n}, S_{i,n})$  by minimizing the least square sum

$$E(A, B_n, T_1^*) = \sum_{n=1}^3 \sum_{i=1}^{k_n} \left( S_{i,n} - \left( A - B_n e^{-(t_{i,n}/T_1^*)} \right) \right)^2 \quad (2)$$

with respect to  $A$ ,  $B_n$  and  $T_1^*$ . The parameter  $k_n$  denotes the number of images within the  $n$ th inversion recovery, which here is  $k_1 = 5$  and  $k_2 = k_3 = 3$ . To determine  $T_1$  from the apparent  $T_1^*$  in Eq. (1) the equilibrium magnetization  $M_0$  is required,

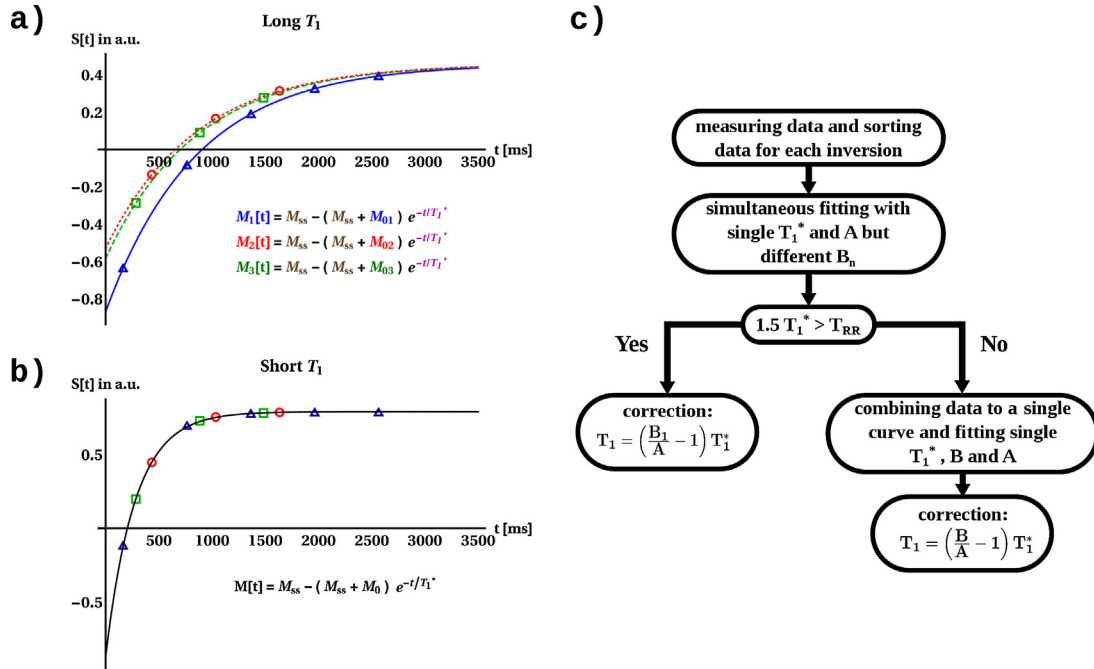


Figure 1. Scheme of the proposed post-processing. Right side: work-flow of the proposed algorithm. Upper left side: for long relaxation times each inversion has a different  $M_{0i}$  and is hence fitted with a different  $B_n$ , but all inversions have the same  $M_{ss}$  (brown), corresponding to the fit parameter  $A$ , and  $T_1^*$  (magenta). This solves the problem of incomplete relaxation before the second and third inversion. Lower left side For short relaxation times only the first signal point in each inversion experiment (labeled by the different colored symbols) deviates significantly from  $M_{ss}$ , This impedes fitting with separate  $B_n$ -values. However, the short  $T_1$  guarantees almost complete recovery of magnetization before subsequent inversions. This makes a single exponential fit (conventional post-processing) to data points of all inversions feasible.

which can be obtained from the initial magnetization after the first inversion pulse (contained in the fitting parameter,  $B_1$ ). i.e.

$$T_1 = \left( \frac{B_1}{A} - 1 \right) T_1^*. \quad (3)$$

### Conditional switch between MOLLI and IGF

IGF works well for long  $T_1$ , or more precisely  $T_1^*$ , where the signal intensities after each inversion recovery experiment cover the dynamic range of the relaxation process (Fig. 1, upper left). However for shorter  $T_1/T_1^*$ , almost only the initial signal intensities obtained after the inversion pulse differ significantly from the steady state values, i.e. the dynamic range of relaxation after an inversion pulse lacks of sampling points which implies a poor fit precision (Fig. 1, lower left). However, as Fig. 1 shows, the standard MOLLI post-processing works well here. The combination of both techniques, standard post-processing for short  $T_1/T_1^*$  and IGF for longer times demands a threshold for switching. Theoretical considerations of the tradeoff between accuracy of the standard -, and precision of the IGF post-processing (see Suppl. and Result section), which were also confirmed by the experiments (Result section) made us set this threshold value to  $T_1^* = T_{RR}/1.5$ . So the algorithm first estimates  $T_1^*$

according to the IGF algorithm. For values above the threshold the IGF algorithm is completed and  $T_1$  obtained from Eq. (3). Values below the threshold demand reevaluation according to the standard post-processing and  $T_1$  derives from Eq. (1) (see Fig. 1).

### Estimation of the error at the switching point

We recently developed an analytical expression for  $T_1^*$  that is obtained by balanced Steady State Free Precession (bSSFP) readouts alternating with undisturbed longitudinal relaxation periods, i.e. the setup of the IGF post-processing [8]. It is a function of longitudinal/transverse relaxation times, parameters of the imaging sequence and heart cycle length,

$$\frac{1}{T_1^*} = \frac{1}{T_1} + \frac{T_{im}}{T_{RR}} \sin\left(\frac{\alpha}{2}\right)^z \left(\frac{1}{T_2} - \frac{1}{T_1}\right) \quad (4)$$

with  $T_1$  as the true value,  $T_{im} = nT_R$  is the duration of the bSSFP readout ( $n$  number of phase encoding steps,  $T_R$  repetition time),  $\alpha$  is the bSSFP flip angle, and  $T_{RR}$  the duration of the heart cycle. In the above equation, we assumed flip back of the spins after the bSSFP readouts.

As this apparent relaxation time and its fitting partner, as well as steady state  $S_{ss}$  and equilibrium magnetization  $S_0$  fulfill

$T_1^*/T_1 = S_{SS}/S_0$ , Eq. (21) in the Suppl. allows the determination of the relative systematic error for the standard MOLLI post-processing as a function of the true  $T_1$  and heart cycle length  $T_{RR}$ .

### Experimental validation

All measurements were performed on a 1.5T clinical scanner (ACHIEVA, Philips Healthcare, The Netherlands). An agarose gel phantom (Agarose2.5%) Type I A-6013, Sigma–Aldrich containing 7 tubes doped with different concentrations of Gadobutrol (Bayer Healthcare, Gadovist;  $T_1$ : 220–2500 ms) was used. Reference  $T_1$  measurements were performed using a saturation recovery spin echo sequence (TE 2.4 ms, TR 5 ms, flip angle  $15^\circ$ , FOV  $250 \times 250$  mm, voxel size 1.60/1.91/10.00 mm) with multiple delay times after the inversion  $T_D$  (25, 50, 100, 125, 200, 250, 300, 500, 1000, 1250, 1500, 2000, 2500, 3000, 4000, 5000 ms).

A 2D-MOLLI sequence provided as a research prototype by the vendor with the acquisition Scheme  $5(n)3(n)3$  was used with  $n$  as the number of heart beats between the inversion experiments (waiting time  $n=0, 1, 2, 3, 4, 10$ ). Multiple RR-intervals (40, 60, 70, 80, 100 bpm) were simulated to investigate the influence of the heart rate. The sequence parameters are: FOV  $370 \text{ mm} \times 370 \text{ mm}$ , bandwidth 1.7 kHz/Pixel, acquisition matrix  $192 \times 190$ , reconstruction matrix  $384 \times 384$  TR 2.4 ms, sense factor 2.3, flip angle  $35^\circ$ , 70 k-space lines, slice thickness 10 mm. We used a linear acquisition profile and a hyperbolic secant pulse.

For each MOLLI post-processing algorithm the mean ( $T_{1,MOLLI}$ ) and standard deviation (SD) of  $T_1$  are calculated from ROIs of the tubes. The relative error of the post-processing as a measure of accuracy was obtained from

$$Error = \frac{T_{1,MOLLI}}{T_{1,SR}} - 1, \quad (5)$$

With  $T_{1,SR}$  as the mean  $T_1$  obtained from the reference (saturation recovery) experiment. The precision of the post-processing algorithms was quantified by its coefficient of variation (relative standard deviation) as

$$relSD = \frac{SD}{T_{1,MOLLI}}. \quad (6)$$

### In vivo validation

The in vivo validation was performed on one healthy volunteer (male, 35 years old) and a series of five consecutive patients aged 24–65 years who were referred to the cMRI department for detection of structural heart disease or acute myocardial damage. All participants were scanned with a 2D-MOLLI as described above prior and after administration of

Gadobutrol (Bayer Healthcare, Gadovist). In the healthy volunteer, we chose  $n$  from 0 to 4, in the patients series we use  $n=1$  and 3.

### Clinical application

According to the recommendations of the SCMR, we acquired a group of 10 patients with normal MRI results that served as reference group (7 males, mean age 45 years (27–72, SD 16)) [9]. Additionally, we included patients who were referred to the cMRI department either for further workup of suspected DCM (12 patients, 11 male patients, mean age 58 years old (34–80, SD 15)) or cardiac amyloidosis (7 patients, 5 male patients, mean age 64 years old (48–82, SD 12)). Of the latter 19 patients, all had presented with an impaired cardiac function, shortness of breath or overall severely impaired clinical status.

We used the 2D MOLLI  $5(1)3(1)3(1)$  both pre- and post-contrast agent administration, and data were analyzed according to the presented adapted algorithm. Gadobutrol 1.0 mmol/ml (Bayer Healthcare, Gadovist) was used as contrast agent, with 1.5 mmol per kg body weight for each patient. Post contrast measurements were performed 13–15 min after contrast agent application. Three MOLLI slices per patient were acquired, with a basal, mid-basal, and apical position. The MOLLI data were processed offline in MATLAB using an external workstation according to the optimized protocol. The calculation of the ECV used a hematocrit-based correction according to prior established protocols [10,11],

$$ECV = (1 - hct) \frac{(1/T_{1_{Myo\ post}} - 1/T_{1_{Myo\ pre}})}{(1/T_{1_{Blood\ post}} - 1/T_{1_{Blood\ pre}})}. \quad (7)$$

All participating individuals have given written informed consent. The local ethics committee has approved the study concept.

## Results

### Phantom validation

Fig. 2 shows the relative errors of  $T_1$  determined by different post-processing strategies compared to the gold standard (saturation recovery method) for 3 phantoms covering a range from moderately short to long  $T_1$  values. For moderate short  $T_1$  (391 ms) all post-processing methods provide similarly accurate results, in particular all are independent from the waiting time and heart rate. With increasing  $T_1$  the standard post-processing algorithm exhibits larger deviations for short waiting periods, and congruently for higher heart rates (Note: waiting periods are measured in cycle lengths =  $1/\text{heart rate}$ ). In contrast, the IGF and the conditional switch post-processing yield results that are more accurate.



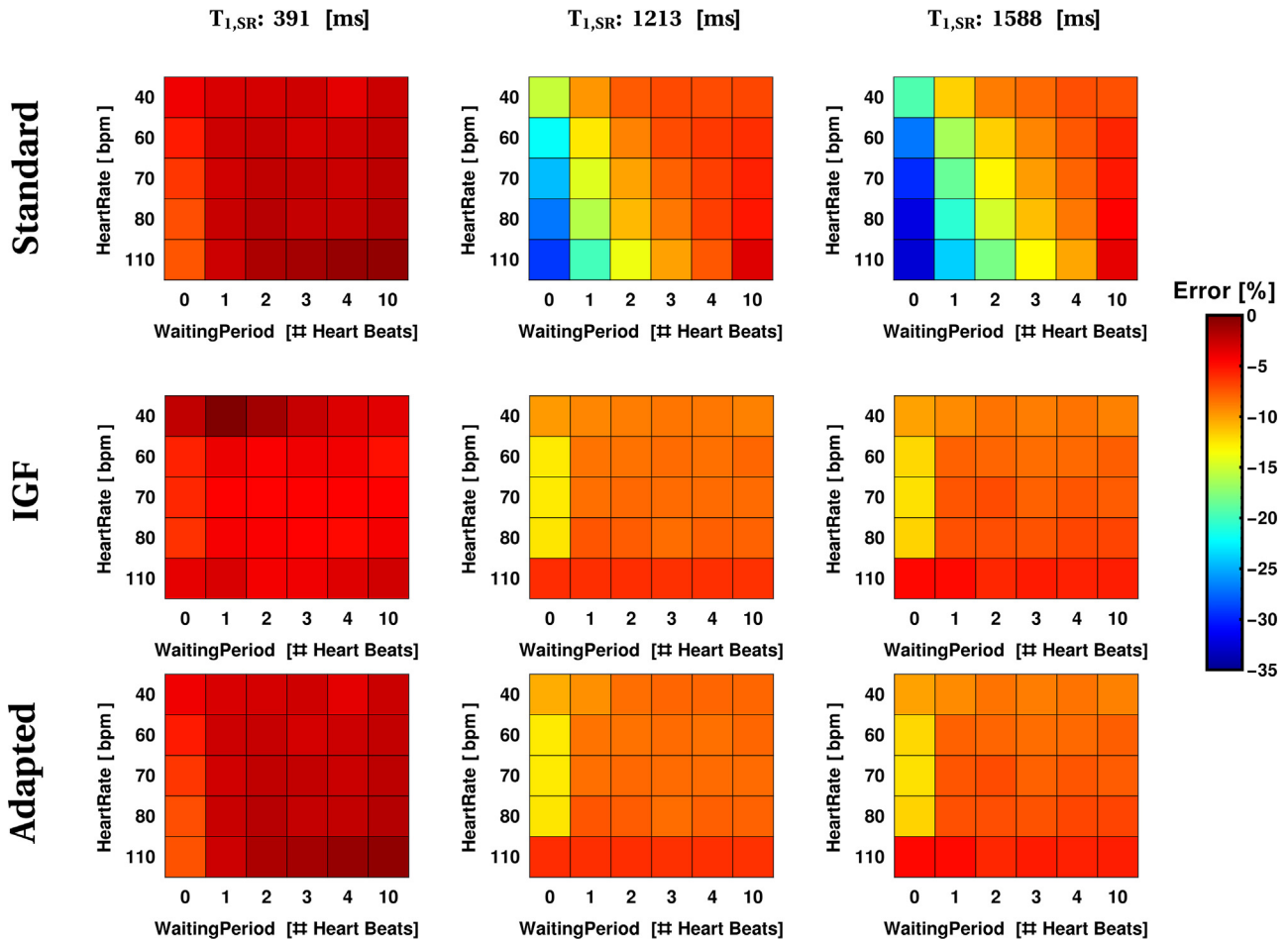


Figure 2. The relative error of  $T_1$  determined from MOLLI data with standard post-processing IGF and the proposed combined post-processing compared to reference measurement using a saturation recovery sequence is presented (see Eq. (7)). To demonstrate the performance of the algorithms for short  $T_1$  the three tubes from the phantom with the shortest  $T_1$  are shown for different heart rates (given in beats per minute – bpm) and waiting times.

Fig. 3 shows the coefficient of variation (ISD/Mean) as a measure of precision for three relaxation times ranging from short to intermediate values and different heart rates. As expected, the longer  $T_1$  the better is the precision for all algorithms. For long  $T_1$  (706 ms) IGF and standard post-processing show comparable coefficients of variation, whereas IGF has significantly less precision (high coefficients) for shorter  $T_1$ . Precision of IGF also decreases with decreasing heart rate, as then many data points are located near the steady state (Fig. 1), which increases the random error for determining  $T_1$ . In contrast the conditional switched (adapted) technique exhibits similar precisions as the standard technique.

#### Estimation of the error at the switching point

For the estimation of the error at the switching point, the waiting time was chosen according to  $t_{wait} = T_{RR}$ , as in

patient scanning. This dependence of the systematic error on relaxation time and heart rate is shown in (Fig. 4), where we assumed a transverse relaxation time of  $T_2 = 50 \text{ ms}$  in myocardium. The solid black threshold line ( $T_1^* = T_{RR}/1.5$ ) exhibits a bias of less than  $\sim 5\%$ . When we take into account that the bias of the standard post-processing algorithm and random error of the IGF algorithm are identical at the threshold (see Suppl.) we estimate  $T_1$  obtained from  $T_1^*$  according to the IGF algorithm to lie in the range  $T_1(1 \pm \text{Error})$ . Eq. (7) determines the corresponding range of  $T_1^*$ . Now, we assume we had by random error determined a  $T_1^*$  at the lower range, which according to the switch algorithm in (Fig. 1) would imply a standard post-processing, whereas the true  $T_1^*$  would have implied the IGF algorithm. The dashed line in Fig. 4 shows the bias of this “wrong” decision, which is also acceptable small about 7%.

This small error near the switching threshold is also obtained from experimental data as shown in (Fig. 5). Both the difference of  $T_1$  obtained from IGF and standard

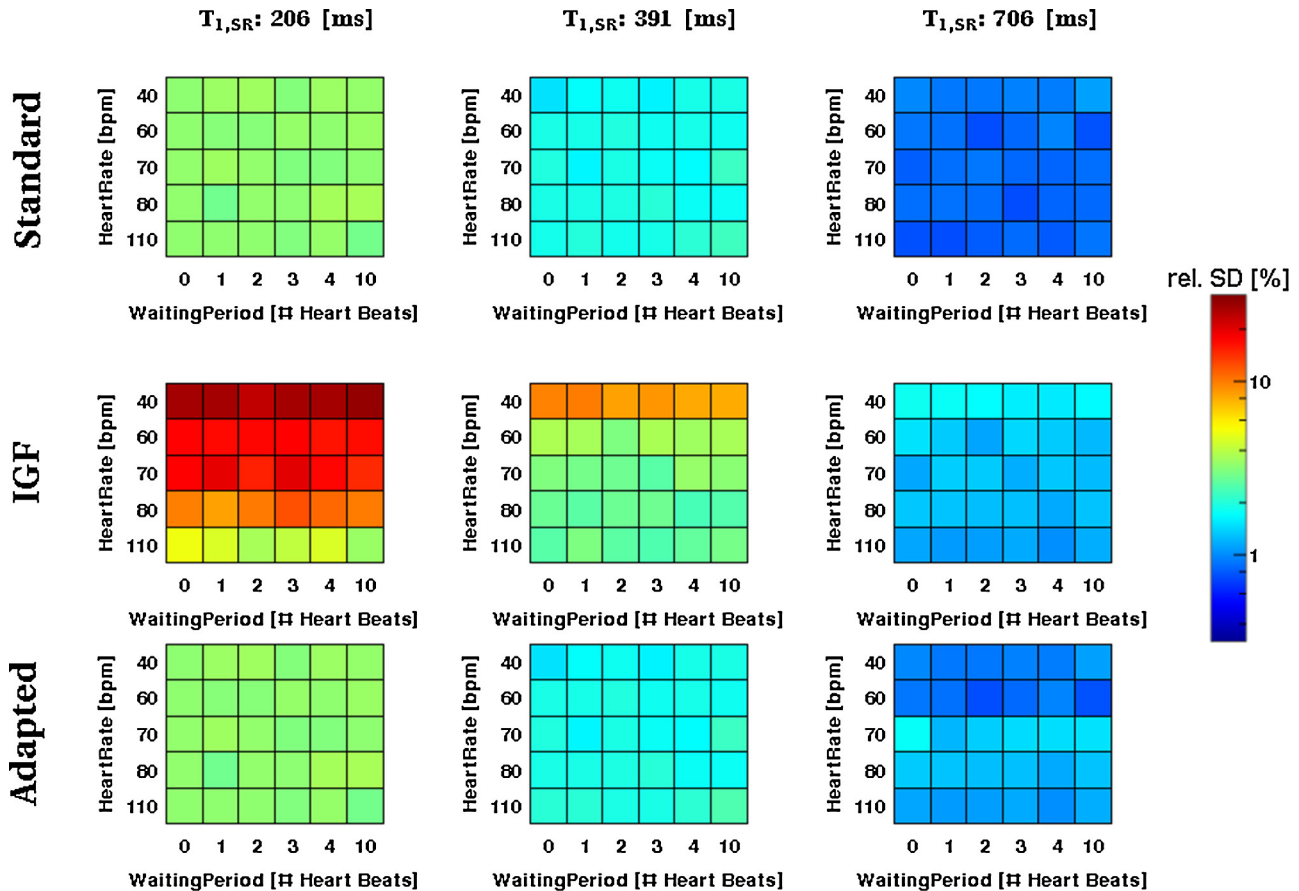


Figure 3. The coefficient of variation (ISD/Mean) of the estimated  $T_1$  determined from MOLLI data with standard post-processing, IGF and the proposed combined post-processing are shown for the tubes with the three shortest relaxation times. The quality of the fitted data is shown for different heart rates (given in beats per minute – bpm) and waiting times.

post-processing, as well the relative random error is in the theoretical predicted range.

### In vivo validation

In vivo  $T_1$ -mapping using the adapted post-processing demonstrated that the calculated  $T_1$  value (red squares in Fig. 6, right) was independent from the waiting period and heart rate. In contrast the  $T_1$  value obtained from the standard post-processing (blue diamonds in Fig. 6) increased with the waiting period and approached asymptotically that of the adapted post-processing after 2–3 heartbeats (Fig. 6, right).

Fig. 7 shows  $T_1$ , obtained from standard and adapted post-processing of intracavitary blood and a septal ROI of myocardium prior to the administration of the contrast agent for two different waiting times. The switching algorithm of the adapted post-processing implied that the long  $T_1$  values were all analyzed by IGF algorithm. This adapted post-processing technique showed no or if at all moderate dependence on waiting time. As expected, the standard procedure systematically underestimated  $T_1$  for the short waiting period. In detail: In the

myocardial ROI the differences of  $T_1$  of the MOLLI 5(1)3(1)3 and MOLLI 5(3)3(3)3 sequence when analyzed according to the standard post-processing sequence reached up to 100 ms, whereas the differences reached not more than 22 ms when using the adapted post-processing method. In the blood ROI the  $T_1$  times differed by a maximum of 185 ms in the standard post-processing method and by a maximum of 101 ms in the adapted post-processing method.

### Clinical application

A total of 53 out of 493 segments according to the AHA 17 segment heart model were excluded due to coregistration artifacts.

The patient group that served as reference group showed a mean ECV of 25% (18–33%; SD = 0.03) in all analyzed slices. The analysis of the clinical scans had excluded any hints for structural or inflammatory diseases of the myocardium.

The analysis of the MRI scans in the DCM group revealed no scars suggesting an ischemic damage (Fig. 8). However, four patients had patchy left ventricular fibrosis. The left

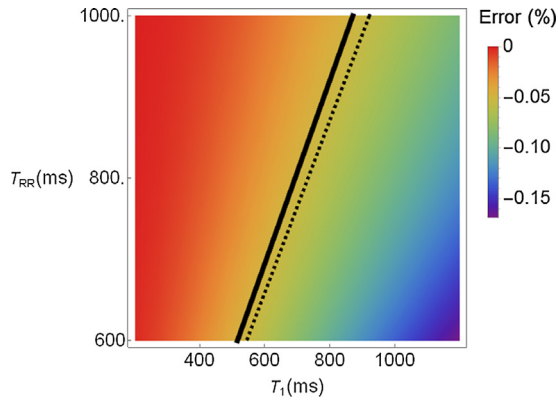


Figure 4. Color-coded bias (relative systematic error) of the standard post-processing algorithm as a function of heart cycle length  $T_{RR}$  and longitudinal relaxation time  $T_1$  as obtained from Eq. (7) and Eq. (21, Suppl.). The solid black line indicates the threshold of switching,  $T_1^* = T_{RR}/1.5$ , the dashed line that of erroneously switching towards standard post-processing by assuming a smaller  $T_1$  due to its random error (see text). Note that bias and random error are equivalent at the switching threshold (Suppl.). Sequence parameters were:  $\alpha = 35^\circ$ , repetition time  $T_R = 2.4$  ms, 86  $\alpha$  pulses, i.e.  $T_{im} = 86 \times 2.4$  ms = 206.4 ms.

ventricular ejection fraction (EF) was measured between 20 and 50% (mean EF 34%, SD 0.09) at the time of the MRI scan. The mean ECV of all analyzed slices is 30% with a range of 22–40% (SD 0.04). The pre contrast mean  $T_1$  was 991 ms [905–1110 ms], the post contrast mean  $T_1$  was 437 ms [393–498 ms]. In the cardiac amyloidosis group the cardiac systolic function was within the normal range, with a measured LV function from 56 to 66% (mean 58%, SD 0.07) at the time of the scans, even though the wall motion was stiff. Overall, the mean ECV was 45% with a range of 30–60% (SD 0.9), the pre contrast mean  $T_1$  was 1060 ms [816–1180 ms] and the post contrast mean  $T_1$  was 378 ms [308–456 ms] (Fig. 9). Higher ECV values were obtained in the basal and midbasal slices again matching the affection in the LGE scans (Table 1).

## Discussion

The intention of the presented work is to demonstrate the validity of an adapted post-processing algorithm that uses both the conventional and the newly suggested IGF post-processing method for the improved determination of  $T_1$  times. This technique aimed to work at the shortest possible breath-hold duration for both short and long  $T_1$  times. All methods, the standard procedure, IGF, as well as the adapted algorithm were

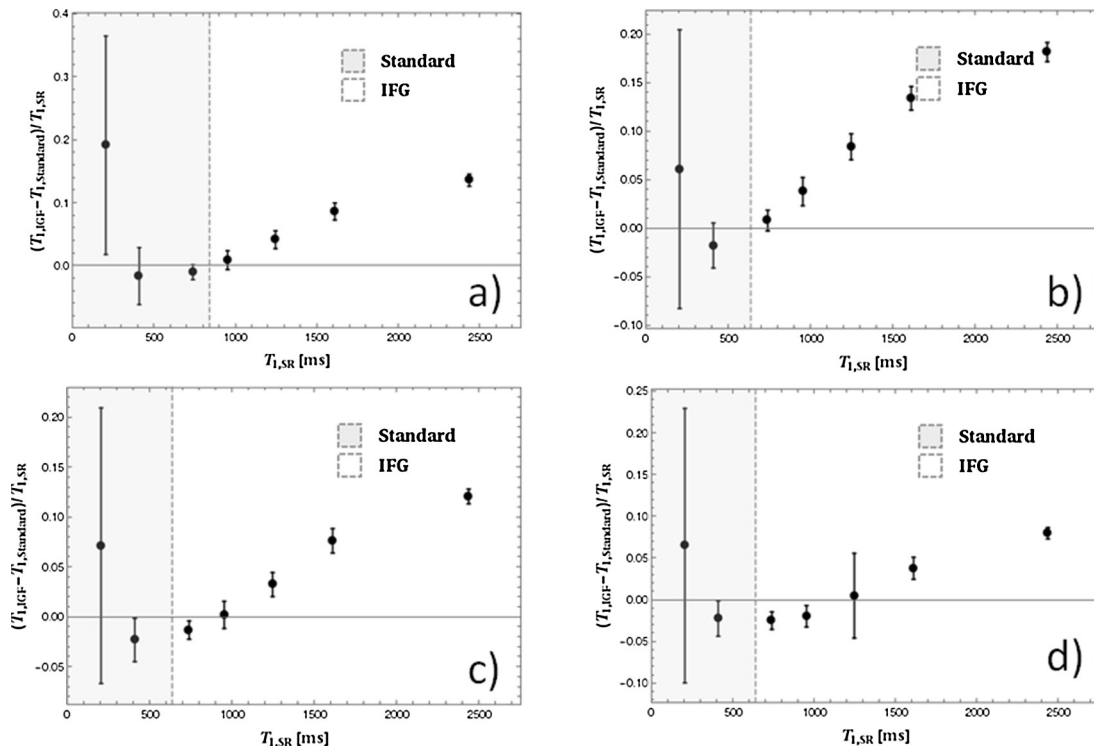


Figure 5. Difference of  $T_1$  values as obtained by IGF and standard post-processing, normalized to  $T_1$  provided by the gold standard (saturation recovery spin-echo sequence). According to the algorithm in Fig. 1, the range of  $T_1$  analyzed with the standard post-processing is shaded in grey, whereas the complement is analyzed with IGF. Different heart rates, and waiting times are considered. Waiting time =  $1T_{RR}$ , HR = 60 bpm (a), 80 bpm (b). HR = 80 bpm, waiting time =  $2T_{RR}$  (c), and  $=3T_{RR}$  (d).

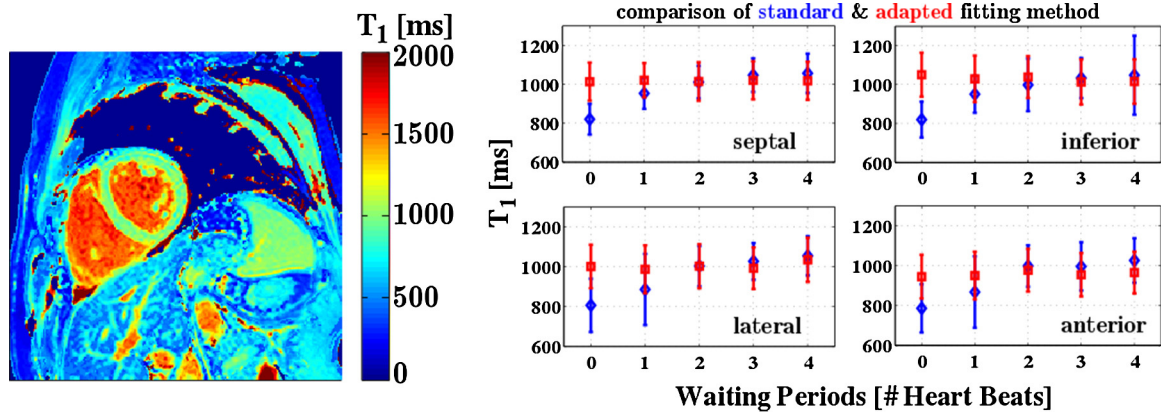


Figure 6. Results of the in vivo validation. (Left) Example of a  $T_1$  map of a healthy volunteer. (Right) Comparison of the relaxation times determined by the standard post-processing (blue diamonds) and the adapted post-processing (red squares) for a total of four ROIS in the myocardium and different waiting periods.

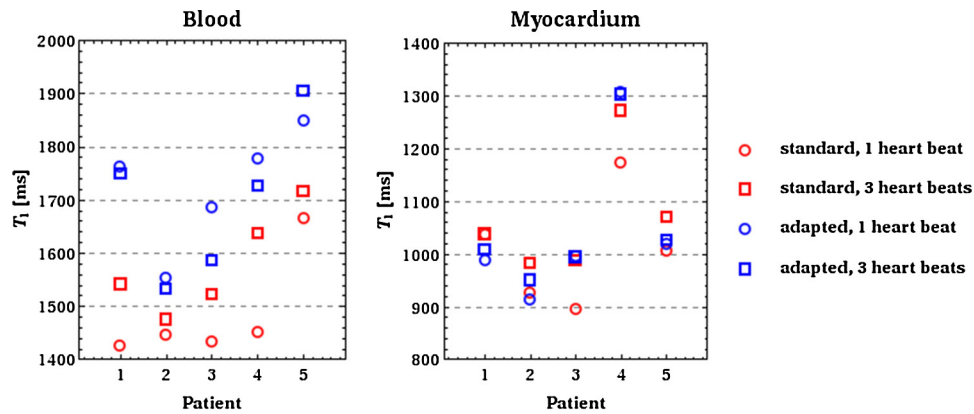


Figure 7. Validation series in 5 patients –  $T_1$  times prior to CA administration in the blood (left figure) and the myocardium (septal ROI, right figure). The  $T_1$  times in the intracavitary blood and myocardium are acquired for different waiting periods (heart beats), MOLLI 5(1)3(1)3 and MOLLI 5(3)3(3)3 and analyzed both by the standard post-processing method and the adapted post-processing method.

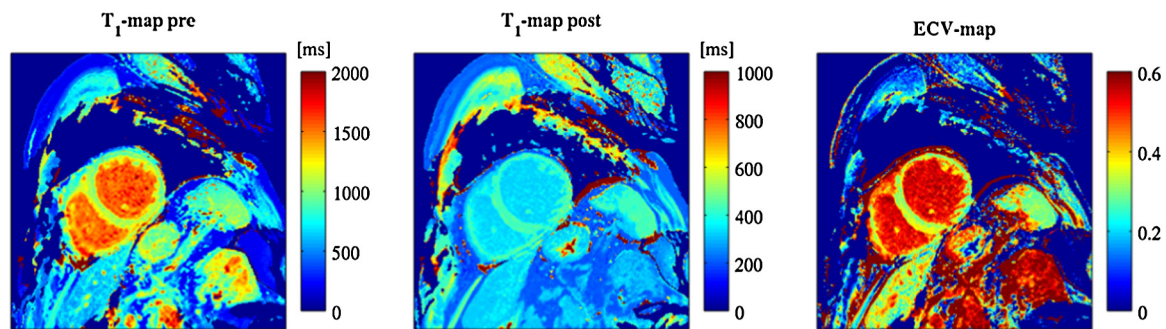


Figure 8. Patient with DCM. Left:  $T_1$  map pre CA administration. Middle:  $T_1$  map post CA administration. Right: corresponding ECV map.

validated in phantom experiments against a gold standard for  $T_1$  measurement with a saturation recovery SE experiment.

The phantom tests show that the  $T_1$ -quantification with standard MOLLI post-processing depends on the real  $T_1$  value, heart rate and the length of the waiting period between the different shots. For long  $T_1$  the standard procedure

systematically underestimates the real  $T_1$  for short waiting time. This is due to an incomplete recovery of the magnetization between inversion experiments. The subsequent inversion pulse results in a reduced inverted magnetization, and the relaxation is apparently accelerated. This effect disappears or is reduced for sufficiently short relaxation



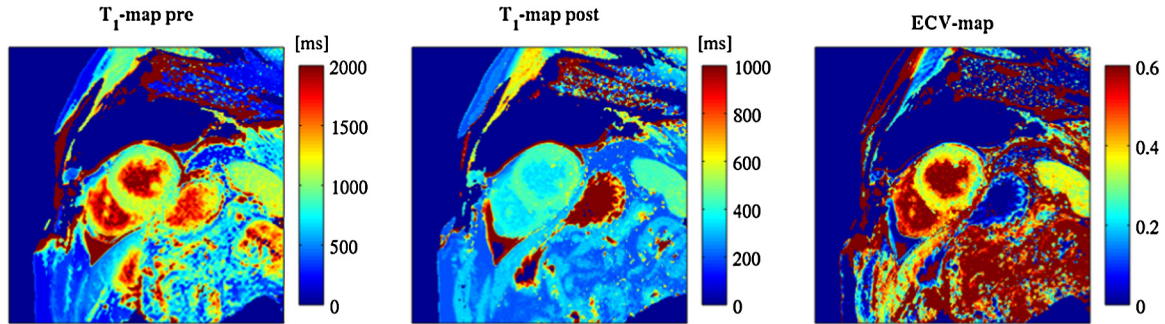


Figure 9. Patient with amyloidosis. Patient with DCM. Left:  $T_1$  map pre CA administration. Middle:  $T_1$  map post CA administration. Right: corresponding ECV map.

Table 1

Myocardial  $T_1$  values pre and post contrast administration and calculated ECV in the reference group, DCM and amyloidosis patients. In brackets, the minimum, maximum and standard deviation are given.

	Myocardial pre $T_1$ (min–max; SD) [ms]	Myocardial post $T_1$ (min–max; SD) [ms]	Myocardial ECV (min–max; SD) [ms]
Reference group			
Basal	704 (883–1023; 52)	455 (407–496; 28)	0.26 (0.29–0.29; 0.03)
Mid-basal	937 (829–1004; 58)	433 (362–481; 40)	0.26 (0.23–0.29; 0.02)
Apical	936 (829–1040; 70)	431 (318–490; 52)	0.25 (0.19–0.31; 0.03)
DCM			
Basal	991 (905–1111; 57)	426 (394–461; 24)	0.32 (0.27–0.40; 0.04)
Mid-basal	984 (905–1058; 49)	441 (401–473; 25)	0.30 (0.22–0.36; 0.04)
Apical	998 (921–1091; 54)	445 (393–498; 28)	0.36 (0.25–0.40; 0.04)
Amyloidosis			
Basal	1063 (816–1179; 117)	367 (316–456; 46)	0.48 (0.33–0.49; 0.09)
Mid-basal	1069 (983–1176; 69)	382 (308–449; 46)	0.44 (0.34–0.52; 0.07)
Apical	1050 (930–1149; 90)	386 (328–439; 42)	0.44 (0.30–0.60; 0.10)

times, because for relaxation times shorter than the RR-cycle magnetization has almost reached its equilibrium value after one inversion experiment.

The IGF allows the reliable quantification of native  $T_1$  times that is less susceptible from the waiting time. However, at least one heart beat waiting time should be maintained because a moderate deviation of less than 3% from the real  $T_1$  was sometimes observed for heart rates of 60, 70, and 80 bpm at a waiting time of zero. Phantom experiment analysis attributed this to an incomplete inversion based on deviations in the inversion pulse that technically cannot be influenced. The incomplete inversion causes an increased bias in the quantified  $T_1$  values especially for short  $T_1$  values. However as this deviation is small it can be neglected in our setting.

Other MOLLI modifications with a shortened acquisition time are in use such as a 5(3)3/4(1)3(1)2 pattern for pre/post contrast  $T_1$  measurements, that shorten the scan time from 17 to 11 heart beats. However, this shortened scan time is achieved by both a shortening of waiting time as well as a reduction in the acquisition of data points that then can be used for the fit routine. Another approach to reduce the systematic

error of  $T_1$  mapping when trying to reduce the waiting time is the ShMolli approach, that uses the 5(1)1(1)1 scheme [12]. Whereas we depend on one threshold for switching between IGF and the standard postprocessing of MOLLI, the postprocessing of ShMolli depends on two thresholds. As our Suppl. shows, even the introduction of one threshold depends on an extensive and lengthy analysis of random and systematic error. The introduction of another threshold would escalate the analysis further. A principle difference is that with IGF, always all relaxation data from the three inversion experiments are used, either for IGF or the standard postprocessing. ShMOLLI, however differentiates. Depending on the value of  $T_1$ , it takes into account only the data of the first inversion for long  $T_1$ , of two inversions for the intermediate and of all three only for short  $T_1$ . As we use more data points for long and intermediate  $T_1$  our approach should have a lower random error.

The MOLLI 5(1)3(1)3 scheme was chosen for all patient measurements. This allowed the reduction of the breath-hold time by four heart beats from 17 to 14 heart beats, while upholding the original number of data point acquisitions. A series of 19 patients who presented with shortness of breath

and an overall reduced physical condition was successfully analyzed using the adapted post-processing algorithm. The participating patients managed a good expiratory compliance resulting in only a small number of segments that had coregistration artifacts that prevented analysis. This result was not influenced by any coregistration algorithms. The measured  $T_1$  times pre and post contrast administration and the calculated ECV values can be matched with recent findings from other groups who used MOLLI for the tissue characterization in DCM and cardiac amyloidosis as well as for normal reference values. Sado et al. measured a mean ECV value in normal individuals of 25.3%, matching a normal ECV of 25.4% according to Kellmann et al. [13,14]. In cardiac amyloidosis, ECV values up to 40% have been reported, whereas in DCM ECV values up to 31% have been documented [15–18]. Our findings show a good congruency with this data.

## Limitations

It must be emphasized that the new post-processing only corrects if necessary for the imperfect inversions in the second and third inversion caused by too short waiting times. It cannot correct for the  $T_2$  and magnetization transfer (MT) dependence of  $T_1^*$  due to the used bSSFP imaging module. These inherent deviations require a different correction scheme which includes these parameters. The presented fitting routine does not solve any arrhythmia-induced problems because it is based on a periodic data acquisition that is identical for the standard post-processing. Due to the limited patient numbers and the focus on the sequence evaluation, we do not perform any evaluation with regards to the clinical outcome or prognostic value of the clinical data.

## Conclusion

We present a post-processing algorithm that uses both the IGF and the standard post-processing algorithm. The modification of the post-processing strategy allows shortening of the measurement time without changes in the established sequence protocol, over the full range of relaxation times present in both native and post CA  $T_1$ -mapping. The protocol allows the examination of even severely impaired patients.

## Competing interests

The authors have no competing interests to declare.

## Author contribution

TK developed the presented post-processing algorithm, participated in performing the scans and the analysis, and drafted the manuscript. WRB participated in the design of the study setup, assisted in the development of the

post-processing algorithm and drafted the manuscript. TR designed the study setup, performed the study scans and the patients' post-processing, and drafted the manuscript. All authors read and approved the manuscript.

## Acknowledgements

This work has been financially supported by the DFG (SFB 688) and the German Heart Failure Centre Wuerzburg, DZHI.

## Appendix A Supplementary data

Supplementary data associated with this article can be found, in the online version, at <http://dx.doi.org/10.1016/j.zemedi.2017.07.003>.

## References

- [1] Banyersad SM, Fontana M, Maestrini V, Sado DM, Captur G, Petrie A, et al. T1 mapping and survival in systemic light-chain amyloidosis. *Eur Heart J* 2015;36(4):244–51, <http://dx.doi.org/10.1093/eurheartj/ehu444>.
- [2] Wong TC, Pichler K, Meier CG, Testa SM, Klock AM, Aneizi AA, et al. Association between extracellular matrix expansion quantified by cardiovascular magnetic resonance and short-term mortality. *Circulation* 2012;126(10):1206–16, <http://dx.doi.org/10.1161/CIRCULATIONAHA.111.089409>.
- [3] Messroghli DR, Greiser A, Frohlich M, Dietz R, Schulz-Menger J. Optimization and validation of a fully-integrated pulse sequence for modified look-locker inversion-recovery (MOLLI) T1 mapping of the heart. *J Magn Reson Imaging* 2007;26(4):1081–6, <http://dx.doi.org/10.1002/jmri.21119>.
- [4] Messroghli DR, Radjenovic A, Kozierke S, Higgins DM, Sivanathan MU, Ridgway JP. Modified Look-Locker inversion recovery (MOLLI) for high-resolution T1 mapping of the heart. *Magn Reson Med* 2004;52(1):141–6, <http://dx.doi.org/10.1002/mrm.20110>.
- [5] Sussman MS, Yang IY, Fok K-H, Wintersperger BJ. Inversion group (IG) fitting: A new T1 mapping method for modified look-locker inversion recovery (MOLLI) that allows arbitrary inversion groupings and rest periods (including no rest period). *Magn Reson Med* 2016;75(6):2332–40, <http://dx.doi.org/10.1002/mrm.25829>.
- [6] Reiter T, Kampf T, Bauer WR. Myocardial fibrosis and extracellular volume in DCM -clinical application of an improved post processing strategy of MOLLI based T1 quantification. *Clin Res Cardiol* April 2014;103(Suppl. 1).
- [7] Nekolla S, Gneiting T, Syha J, Deichmann R, Hasse A. T1 maps by K-space reduced snapshot-FLASH MRI. *J Comput Assist Tomogr* 1992;16(2):327–32.
- [8] Kampf T, Reiter T, Bauer WR. An analytical model which determines the apparent T1 for modified look-locker inversion recovery (MOLLI) – analysis of the longitudinal relaxation under the influence of discontinuous balanced and spoiled gradient echo readouts; 2017 [arXiv:1704.06898](https://arxiv.org/abs/1704.06898).
- [9] Moon JC, Messroghli DR, Kellman P, Piechnik SK, Robson MD, Ugander M, et al. Myocardial T1 mapping and extracellular volume quantification: A society for Cardiovascular Magnetic Resonance (SCMR) and CMR Working Group of the European Society of Cardiology consensus statement. *J Cardiovasc Magn Reson* 2013;15:92, <http://dx.doi.org/10.1186/1532-429X-15-92>.
- [10] Flett AS, Hayward MP, Ashworth MT, Hansen MS, Taylor AM, Elliott PM, et al. Equilibrium contrast cardiovascular magnetic resonance for the measurement of diffuse myocardial fibrosis:

- Preliminary validation in humans. *Circulation* 2010;122(2):138–44, <http://dx.doi.org/10.1161/CIRCULATIONAHA.109.930636>.
- [11] Jerosch-Herold M, Sheridan DC, Kushner JD, Nauman D, Burgess D, Dutton D, et al. Cardiac magnetic resonance imaging of myocardial contrast uptake and blood flow in patients affected with idiopathic or familial dilated cardiomyopathy. *Am J Physiol Heart Circ Physiol* 2008;295(3):H1234–42, <http://dx.doi.org/10.1152/ajpheart.00429.2008>.
- [12] Piechnik SK, Ferreira VM, Dall'Armellina E, Cochlin LE, Greiser A, Neubauer S, et al. Shortened Modified Look-Locker Inversion recovery (ShMOLLI) for clinical myocardial T1-mapping at 1.5 and 3 T within a 9 heartbeat breathhold. *J Cardiovasc Magn Reson* 2010;12:69, <http://dx.doi.org/10.1186/1532-429X-12-69>.
- [13] Kellman P, Wilson JR, Xue H, Bandettini WP, Shanbhag SM, Druey KM, et al. Extracellular volume fraction mapping in the myocardium, part 2: Initial clinical experience. *J Cardiovasc Magn Reson* 2012;14:64, <http://dx.doi.org/10.1186/1532-429X-14-64>.
- [14] Sado DM, Flett AS, Banypersad SM, White SK, Maestrini V, Quarta G, et al. Cardiovascular magnetic resonance measurement of myocardial extracellular volume in health and disease. *Heart* 2012;98(19):1436–41, <http://dx.doi.org/10.1136/heartjnl-2012-302346>.
- [15] Banypersad SM, Sado DM, Flett AS, Andrew S, Gibbs SDJ, Pinney JH, et al. Quantification of myocardial extracellular volume fraction in systemic AL amyloidosis: An equilibrium contrast cardiovascular magnetic resonance study. *Circ Cardiovasc Imaging* 2013;6(1):34–9, <http://dx.doi.org/10.1161/CIRCIMAGING.112.978627>.
- [16] dem Siepen F aus, Buss SJ, Messroghli D, Andre F, Lossnitzer D, Seitz S, et al. T1 mapping in dilated cardiomyopathy with cardiac magnetic resonance: Quantification of diffuse myocardial fibrosis and comparison with endomyocardial biopsy. *Eur Heart J Cardiovasc Imaging* 2015;16(2):210–6, <http://dx.doi.org/10.1093/ehjci/jeu183>.
- [17] Hong YJ, Park CH, Kim YJ, Hur J, Lee H-J, Hong SR, et al. Extracellular volume fraction in dilated cardiomyopathy patients without obvious late gadolinium enhancement: Comparison with healthy control subjects. *Int J Cardiovasc Imaging* 2015;31(Suppl 1):115–22, <http://dx.doi.org/10.1007/s10554-015-0595-0>.
- [18] Weingartner S, Akcakaya M, Basha T, Kissinger KV, Goddu B, Berg S, et al. Combined saturation/inversion recovery sequences for improved evaluation of scar and diffuse fibrosis in patients with arrhythmia or heart rate variability. *Magn Reson Med* 2014;71(3):1024–34, <http://dx.doi.org/10.1002/mrm.24761>.

Available online at [www.sciencedirect.com](http://www.sciencedirect.com)

**ScienceDirect**